Channel Estimation and Turbo Equalization for Coded OTFS and OFDM: A Comparison

Xiang Huang†, Arman Farhang*, and Rong-Rong Chen†

***Abstract*—In this letter, we study joint channel estimation and turbo equalization for coded orthogonal time frequency space (OTFS) and orthogonal frequency division multiplexing (OFDM). To the best of our knowledge, this is the first study that compares performance of OTFS and OFDM coded systems using the state-of-the-art message passing (MP) and soft minimum mean square error (MMSE) equalizers, under imperfect channel estimation. We show that the commonly used threshold-based channel estimator incurs noticeable performance loss for OTFS. Hence, we propose a basis expansion model (BEM) channel estimation technique for OTFS, which improves performance of the threshold-based channel estimator and yields a superior performance to OFDM when using small modulations of BPSK and QPSK. Our work also reveals that OTFS can perform inferior to OFDM as the modulation order increases. This is due to the increased 2D detection complexity of OTFS.**

***Index Terms*—OTFS, OFDM, turbo equalization, Message Passing, LDPC, BEM, Soft MMSE equalizer**

I. Introduction

Orthogonal frequency division multiplexing (OFDM) as the air interface technology has been very successful in the last two generations of wireless systems. However, it suffers from a significant performance degradation in rapidly time-varying channels due to severe inter-carrier-interference (ICI). Recently, a new waveform called orthogonal time frequency space (OTFS) modulation has stirred a great deal of interests. OTFS was first proposed in [1] as a new modulation scheme where each transmitted symbol experiences a near-constant channel gain even in channels with high Doppler spread. OTFS spreads symbols from the delay-Doppler (DD) domain to the frequency-time (FT) domain using an inverse symplectic finite Fourier transform (ISFFT) operation. This enables OTFS to achieve a full diversity gain even in an uncoded system.

A threshold-based channel estimator that deploys an isolated and high power pilot in the center of the DD domain is widely used in OTFS literature [2]. Despite its simplicity, this estimator has some limitations. First, since the channel estimation is based on a single pilot only, it requires high power which reduces the transmission power available for data transmission. Second, for channels with high Doppler spread, the channel variations across different symbols in the DD domain are not captured using this estimator. To overcome these limitations, we propose a channel estimation technique for OTFS based on the basis expansion model (BEM), motivated by similar approaches in OFDM literature [3]. The proposed approach uses estimated data symbols to iteratively refine channel estimation, which achieves a more accurate channel estimation with a significantly reduced transmission power on pilots. We note that the existing work in [4] considers BEM-based channel estimation combined with compressed sensing for OTFS. The authors in [4] perform channel estimation using frequency domain pilots only and the estimated data symbols are not utilized to refine the channel estimate as in this work.

In this letter, we compare OTFS and OFDM under imperfect channel state information (CSI) while taking into account power allocation between pilot and data transmissions. We adopt the state-of-the-art soft minimum mean square error (MMSE) and message passing (MP) equalizers together with a BEM-based channel estimator for both OTFS and OFDM. This ensures that comparisons are made using the best performance each system can achieve. Besides, we consider coded systems where channel coding is over multiple OFDM symbols. This helps improve the time-diversity of OFDM and hence, make our comparison with OTFS, which intrinsically utilizes the time-diversity of the channel, fair. In comparison to the current work, the existing literature that compare OTFS and OFDM, focus on either uncoded systems [5], [6], or assume perfect CSI [1], [7]. In [1] and [8], a simple linear MMSE equalizer is used for OFDM, which cannot effectively remove ICI.

We summarize the main contributions of this work as:

- To the best of our knowledge, this is the first work to compare OTFS and OFDM systems under the practical settings of (1) imperfect CSI, (2) utilization of channel coding, and (3) powerful equalizers to remove interference for both OFDM and OTFS. Existing comparisons lack in one or more of these aspects and thus, they cannot provide an accurate comparison.
- We find that the commonly used threshold-based channel estimator yields inferior performance when transmission power on pilot is taken into account. We propose a BEM-based channel estimation technique for OTFS that significantly reduces the required pilot power while providing an improved estimation accuracy.
- We obtain encouraging results that reveal the superior performance of coded OTFS to coded OFDM for small modulations of BPSK and QPSK, when our proposed BEM-based channel estimator is utilized. In contrast, we find that for the larger modulation of 16-QAM, due to challenges of 2D detection, the advantages of a coded OTFS system diminish. This suggests the need for development of more advanced equalizers for OTFS to fully unlock the potential of this promising waveform.

Notations: Matrices and vectors are denoted by boldface uppercase and boldface lowercase, respectively. Superscripts $(\cdot)^{\mathrm{T}}$ and $(\cdot)^{\mathrm{H}}$ denote transpose and conjugate transpose operations, respectively. The function $\mathrm{vec}(\mathbf{X})$ vectorizes matrix

Xiang Huang and Rong-Rong Chen are with Dept. of ECE, University of Utah, USA. Arman Farhang is with Dept. of Electronic and Electrical Engineering, Trinity College Dublin, Ireland. This work is supported by NSF Grants 2153875 and 2229562 and also the Science Foundation Ireland under Grants 19/FFP/7005(T) and 21/US/3757.

This article has been accepted for publication in IEEE Wireless Communications Letters. This is the author's version which has not been fully edited and content may change prior to final publication. Citation information: DOI 10.1109/LWC.2023.3284778

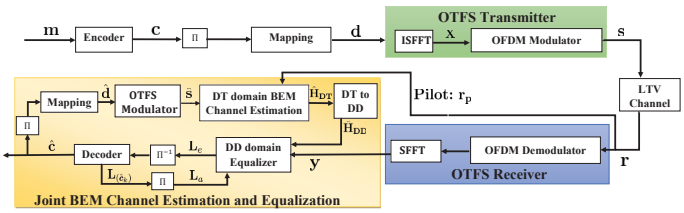

(a) Block diagram of the OFDM-based OTFS system.

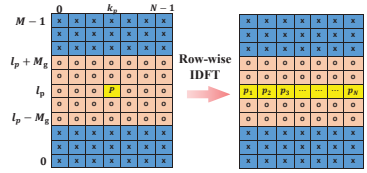

(b) A single pilot in the DD domain (left) corresponds to N time domain pilots after the IDFT (right). Each '×' denotes a data symbol, each '○' denotes a null symbol in the guard band.

Fig. 1: Block diagram of an OFDM-based OTFS system and illustration of pilot pattern.

$\mathbf{X}$ by stacking its columns in a column vector. $\mathbf{I}_m$ and $\mathbf{0}_{m\times n}$ are identity and zero matrices of sizes $m \times m$ and $m \times n$, respectively. $\otimes$ denotes the *Kronecker* product. $\mathbf{F}_M$ is the normalized M-point discrete Fourier transform (DFT) matrix with elements $[\mathbf{F}_M]_{mn} = e^{\frac{-j2\pi mn}{M}}/\sqrt{M}$, for $m,\ n = 0, ..., M-1$.

II. System Model for OFDM-based OTFS

In this section, we describe the OFDM-based OTFS system shown in Fig. 1a. The codeword $\mathbf{c}$ encoded from the message $\mathbf{m}$ is interleaved and mapped to data symbols $\mathbf{d}$ in the DD domain. These symbols are first transformed into the FT domain by the ISFFT block and then sent through the linear time-varying (LTV) channel using the OFDM modulator. At the receiver, the received signal $\mathbf{r}$ is first demodulated and then converted to the DD domain via the SFFT block. Details of the proposed joint BEM channel estimation and equalization block will be explained in detail in Sections III and IV.

To cast the above operations at the transmitter and receiver into the mathematical formulation, let us consider an OTFS system with M delay and N Doppler bins. The DD domain data matrix $\mathbf{D}$ with elements $d_{m,n}$, corresponding to symbols placed in the delay and Doppler bins $m = 0, \ldots, M-1$ and $n = 0, \ldots, N-1$, respectively, can be converted to the FT domain using the ISFFT operation as $\mathbf{X} = \mathbf{F}_M \mathbf{D} \mathbf{F}_N^{\mathrm{H}}$ and $\mathbf{x} = \mathrm{vec}(\mathbf{X})$. This is a 2D Fourier transform operation that converts the delay and Doppler to the frequency and time dimensions, respectively, by taking M-point DFT from the columns of $\mathbf{D}$ and N-point IDFT from the rows of the resulting matrix. The OTFS transmit signal is then formed by passing the FT signal $\mathbf{X}$ into the OFDM modulator as

$$\mathbf{S} = \mathbf{A}_{\mathrm{cp}} \mathbf{F}_M^{\mathrm{H}} \mathbf{X} = \mathbf{A}_{\mathrm{cp}} \mathbf{D} \mathbf{F}_N^{\mathrm{H}}, \tag{1}$$

where $\mathbf{A}_{\mathrm{cp}} = [\mathbf{G}_{\mathrm{cp}}^{\mathrm{T}}, \mathbf{I}_M^{\mathrm{T}}]^{\mathrm{T}}$ is the cyclic prefix (CP) addition matrix, $\mathbf{G}_{\mathrm{cp}}$ is formed by the last M_{cp} rows of $\mathbf{I}_M$, and M_{cp} is the CP length. Finally, the resulting signal, $\mathbf{S}$, in the delay-time (DT) domain according to (1), is converted to a serial stream by concatenating its columns as $\mathbf{s} = \mathrm{vec}(\mathbf{S})$, and it is passed through the wireless channel.

The received signal after transmission over a linear time varying (LTV) channel is $r[i] = \sum_{l=0}^{L-1} h[i,l]s[i-l] + w[i]$, where $h[i,l]$ is the instantaneous channel impulse response (CIR) at time instant i and tap l, L is the channel length, and $w[i]$ is the additive white Gaussian noise (AWGN). The received signal can be written in a vectorized form as $\mathbf{r} = \mathbf{H}_{\mathrm{DT}}\mathbf{s} + \mathbf{w}$, where $\mathbf{H}_{\mathrm{DT}}$ is the delay-time domain convolution matrix with a Toeplitz-like structure that is lower triangular with elements $h[i,l]$ at its l^{th} lower diagonal and i^{th} row. $\mathbf{w}$ is the noise vector formed by the samples $w[i]$. As it is shown in [9], the end-to-end relation for the OTFS is represented as

$$\mathbf{y} = \mathbf{H}_{\mathrm{DD}}\mathbf{d} + \hat{\mathbf{w}}, \tag{2}$$

where $\mathbf{H}_{\mathrm{DD}} = (\mathbf{F}_N \otimes \mathbf{R}_{\mathrm{cp}})\, \mathbf{H}_{\mathrm{DT}} \left(\mathbf{F}_N^{\mathrm{H}} \otimes \mathbf{A}_{\mathrm{cp}}\right)$ denotes the end-to-end DD domain channel, and $\mathbf{R}_{\mathrm{cp}} = [\mathbf{0}_{M\times M_{\mathrm{cp}}}, \mathbf{I}_M]$ is the CP removal matrix.

III. Channel Estimation for OTFS

In this section, we first describe the threshold-based DD domain channel estimation for OTFS. Then, we present our proposed joint BEM-based channel estimator and detector.

A. Threshold-based Channel Estimation

In OTFS modulation, the 2D channel impulse response (CIR) seen by each symbol in DD domain is approximately the same. Thus, it is sufficient to estimate the 2D CIR using a single pilot symbol. As introduced in [2], one can simply place the pilot symbol, denoted as $d[l_{\mathrm{p}}, k_{\mathrm{p}}]$, in the center of the DD grid as shown in Fig. 1b, where l_{p} and k_{p} are the row and column indices of the pilot symbol. To avoid interference to the pilot, zero symbols are placed around the pilot symbol in the guard zone, i.e., $\{d[l,k] = 0, l_{\mathrm{p}} - M_{\mathrm{g}} \le l \le l_{\mathrm{p}} + M_{\mathrm{g}}, 0 \le k \le N-1$ for $l \ne l_{\mathrm{p}}$ and $k \ne k_{\mathrm{p}}\}$, where M_{g} is the number of zero guard symbols around the pilot symbol in the delay dimension. The rest of the grid is filled with data symbols. After being transmitted over the LTV channel and transformed back to the DD domain, the received symbols $\{y[l,k], l_{\mathrm{p}} \le l \le l_{\mathrm{p}} + M_{\mathrm{g}}, 0 \le k \le N-1\}$ are extracted to estimate the 2D CIR, $\{h_{2\mathrm{D}}[l,k], l_{\mathrm{p}} \le l \le l_{\mathrm{p}} + M_{\mathrm{g}}, 0 \le k \le N-1\}$. Therefore, the received symbols $y[l,k]$ are given by

$$y[l,k] = h_{2\mathrm{D}}[l,k] \cdot d[l_{\mathrm{p}}, k_{\mathrm{p}}] + v[l,k], \tag{3}$$

where $l_{\mathrm{p}} \le l \le l_{\mathrm{p}} + M_{\mathrm{g}}, 0 \le k \le N-1$, $v[l,k]$ follows a complex Gaussian distribution with zero mean and variance of N_0. We then estimate the 2D CIR $\hat{h}_{2\mathrm{D}}[l,k]$ as in [2] by letting

$$\hat{h}_{2\mathrm{D}}[l,k] = \begin{cases} y[l,k]/d[l_{\mathrm{p}}, k_{\mathrm{p}}] & \text{if } y[l,k] \ge \mathcal{T}, \\ 0 & \text{Otherwise,} \end{cases} \tag{4}$$

where $\mathcal{T}$ is a pre-determined threshold. Subsequently, under the assumption that approximately the same CIR is seen by each symbol, we can construct $\hat{\mathbf{H}}_{\mathrm{DD}} \in \mathbb{C}^{MN\times MN}$ in (2) from the vectorized version of $\hat{h}_{2\mathrm{D}}[l,k]$ using proper circular shift.

B. Proposed Joint Channel Estimation and Data Detection

As shown in Fig. 1b, by applying the row-wise IDFT, the central pilot symbol in the DD domain is transformed to N time-domain pilot symbols $p_1, \cdots, p_N$, one within each OFDM symbol. The corresponding time domain frame

This article has been accepted for publication in IEEE Wireless Communications Letters. This is the author's version which has not been fully edited and content may change prior to final publication. Citation information: DOI 10.1109/LWC.2023.3284778

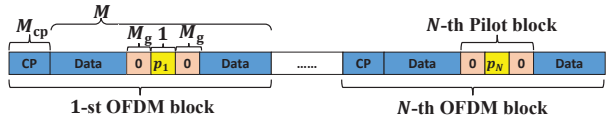

(a) OFDM-based OTFS frame structure

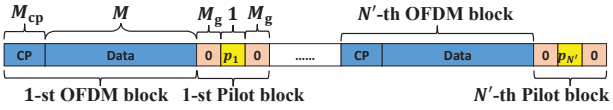

(b) OFDM frame structure

Fig. 2: Frame structures for OTFS and OFDM.

structure is shown in Fig. 2 (a), where a pilot block, consisting of one pilot symbol, surrounded by $2 \times M_g$ zero symbols, is placed in the center of each OFDM block. Interestingly, this frame structure resembles a time-domain OFDM structure shown in Fig. 2 (b). The latter was used in [3] for time-domain channel estimation of an OFDM system using BEM model. Given the similarity of the frame structures, we are motivated to extend BEM channel estimation to the OFDM-based OTFS system to improve channel estimation accuracy. The key idea is to convert symbol estimates from the DD to DT domain to facilitate BEM channel estimation.

We describe details of our proposed BEM channel estimation for OTFS as follows. Let $N = K_{\rm t} \times K_{\rm b}$, where $K_{\rm t}$ is the number of transmission blocks and each consists of $K_{\rm b}$ OFDM blocks. As in [3], we perform channel estimation over each transmission block. BEM channel estimation is applied to estimate coefficients of the l-th tap over the duration of a transmission block, denoted by $\mathbf{h}_l = [h[\kappa, l], h[\kappa+1, l], \cdots h[\kappa + M^* - 1, l]^T$. Here, $M^* = (M + M_{\rm cp}) \times K_{\rm b}$ is the number of data symbols in each transmission block, and κ is the starting time of the transmission block. Specifically, using $\mathcal{B}$ basis expansion functions, we approximate $\mathbf{h}_l$ by $\hat{\mathbf{h}}_l = \mathbf{E}\mathbf{v}_l$, where $\mathbf{E} = [\mathbf{e}_1^T, \cdots, \mathbf{e}_{M^*}^T]^T \in \mathbb{C}^{M^* \times \mathcal{B}}$ is the BEM matrix. Each row of $\mathbf{E}$, given by $\mathbf{e}_m = [E_0(m) \cdots, E_{\mathcal{B}-1}(m)] \in \mathbb{C}^{1 \times \mathcal{B}}$, represents samples of the $\mathcal{B}$ basis functions at the m-th data symbol. The BEM coefficient vector $\mathbf{v}_l = [v_0, ..., v_{\mathcal{B}-1}]^T \in \mathbb{C}^{\mathcal{B} \times 1}$ for tap l will be updated for each transmission block.

The proposed BEM-based OTFS receiver is illustrated in Fig. 1a. The initial $\mathbf{v}_l$, $l = 0, \cdots, L-1$ is calculated based on received pilot signals $\mathbf{r}_{\rm p}^i = [r[\rho_i], r[\rho_i + 1], \ldots, r[\rho_i + M_g]]^{\rm T}$ only, where ρ_i is the index of the single pilot in the $i^{\rm th}$ pilot block, and follow the Kalman filter updates [3]. To update $\mathbf{v}_l$ after each equalization and decoding iteration, we first interleave the hard decision $\hat{\mathbf{c}}$, and then remap it to obtain the DD domain transmit symbol estimates $\hat{\mathbf{d}}$. By taking the OTFS modulation, $\hat{\mathbf{d}}$ is transformed to $\hat{\mathbf{s}}$ in the DT domain. Together with the received DT domain signals $\hat{\mathbf{r}}$, $\hat{\mathbf{s}}$ is then fed to channel estimation block to update the measurement matrix in the Kalman filter. Considering the estimated data symbols in addition to known pilot symbols, we fine tune the estimate of $\hat{\mathbf{H}}_{\rm DT}$ and derive $\hat{\mathbf{H}}_{\rm DD}$ based on (2). The latter will be used in the next iteration of turbo equalization.

IV. Turbo Equalization

In this work, we consider two equalizers– the soft MMSE equalizer and the MP equalizer [5]. To the best of our knowledge, the performance of these two equalizers have not been compared in the literature for OTFS or OFDM systems under the setting of channel estimation and turbo equalization.

As shown in Fig. 1a, for OTFS, the inputs to the equalizer include channel estimate $\hat{\mathbf{H}}_{\rm DD}$ from (2), signal $\mathbf{y}$, and *a priori* Log-Likelihood Ratio (LLR) $\mathbf{L}_a$ for the coded bits; the outputs are extrinsic LLR $\mathbf{L}_e$. The soft MMSE equalizer utilizes *a priori* mean and variance of the coded symbols, calculated from $\mathbf{L}_a$, to determine the linear filter coefficients and then from which extrinsic LLR $\mathbf{L}_e$ are computed assuming a Gaussian distribution on the symbol *a posteriori* probabilities $P(\hat{d}_{m.n}|\mathbf{y}, \mathbf{L}_a, \hat{\mathbf{H}}_{\rm DD})$. Over joint channel estimation, equalization, and channel decoding iterations, as the estimated bits from the decoder improve, the quality of the channel estimates also improves. This leads to an improved equalization.

In an MP equalizer [5], Eq. (2) is modeled as a sparsely connected factor graph based on $\hat{\mathbf{H}}_{\rm DD}$, where NM variable nodes correspond to $\mathbf{d}$ and NM observation nodes correspond to $\mathbf{y}$. Each iteration of the message update utilizes the most recent messages passed from other parts of the graph. In comparison, the soft MMSE equalizer assumes a fixed prior during each equalization step. As shown in Section V, the iterative message updating in the MP equalizer holds certain advantages over the soft MMSE equalizer when $\hat{\mathbf{H}}_{\rm DD}$ is sparse, but may perform inferior when $\hat{\mathbf{H}}_{\rm DD}$ is dense, due to increased correlation in the messages.

V. Simulation Results

A. System Parameters

We apply channel coding to both systems under study. For OTFS, channel coding is done for each OTFS block, consisting of N OFDM symbols. Similarly, for OFDM, channel coding is also across N' consecutive OFDM symbols. Since the frame structures of the two systems are different (see Fig. 2), N and N' are chosen such that we can use a channel code of the same length for both systems. The transmitted average energy per information bit to noise power ratio, denoted by $E_{\rm b}/N_0$, is defined as $\frac{E_{\rm b}}{N_0}({\rm dB}) = 10\log_{10}\left(\frac{E_{\rm s}}{RN_0}\right)$, where $E_{\rm s}$ is the average energy per symbol and R is the transmission rate.

For OTFS, we assume that each data symbol has an average energy of $E_{\rm d}$, and the single pilot symbol shown in Fig. 1b has an energy of $E_{\rm p}$. Then we calculate the average energy per symbol, denoted by $E_{\rm s}^{\rm OTFS}$, as

$$E_{\rm s}^{\rm OTFS} = \frac{(M - 2M_{\rm g} - 1) \times N \times E_{\rm d} + M_{\rm cp} \times N \times E_{\rm d} + E_{\rm p}}{(M + M_{\rm cp}) \times N}, \tag{5}$$

where $M_{\rm cp}$ is the length of cyclic prefix and $M_{\rm g} = M_{\rm cp} - 1$ is the one-side guard length along the delay dimension. In (5), the guard zone is spanned across the entire doppler dimension. Based on this assumption, the transmission rate is defined as

$$R^{\rm OTFS} = r_{\rm c} \cdot \frac{M - (2M_{\rm g}) - 1}{M + M_{\rm cp}} \cdot \log_2 Q, \tag{6}$$

where $r_{\rm c}$ is the channel code rate, Q is the modulation size.

In comparison, using the pilot pattern shown in Fig. 2(b), we define $E_{\rm s}^{\rm OFDM}$ and the transmission rate $R^{\rm OFDM}$ as

$$E_{\rm s}^{\rm OFDM} = \frac{(M + M_{\rm cp}) \times N' \times E_{\rm d} + E_{\rm p}}{(M + M_{\rm cp} + 2M_{\rm g} + 1) \times N'}. \tag{7}$$

$$R^{\rm OFDM} = r_{\rm c} \cdot \frac{M}{M + M_{\rm cp} + 2M_{\rm g} + 1} \cdot \log_2 Q \tag{8}$$

This article has been accepted for publication in IEEE Wireless Communications Letters. This is the author's version which has not been fully edited and content may change prior to final publication. Citation information: DOI 10.1109/LWC.2023.3284778

TABLE I: Simulation Parameters

sub-carrier spacing: 10KHz, # of BEM coefficients: $\mathcal{B}=9$				
	OTFS(OFDM)			
Setting	1	2	3	4
Mod	BPSK	QPSK	QPSK	16-QAM
M	128(128)	128(128)	64(64)	64(64)
$N(N')$	32(27)	32(27)	60(39)	60(39)
$K_{\rm b}$	8(8)	8(8)	15(13)	15(13)
$K_{\rm t}$	4(3)	4(3)	4(3)	4(3)
R	0.375(0.380)	0.750(0.760)	0.539(0.646)	1.079(1.293)
code	(10,20,168)	(10,20,336)	(10,20,246)	(10,20,492)
PAPR	7.91(7.64)	7.76(7.99)	7.83(7.91)	7.77(7.85)

* *Note*: Setting pairs $(1,2)$ and $(3,4)$ have different alphabet sizes with the same M and N. Four rate $1/2$ 5G-QC-B-LDPC codes of length $N_B \times Z$ with parameters (M_B, N_B, Z) are used, where M_B and N_B are row number and column number of base matrix, and Z is the expansion factor. PAPR in dB values are calculated through simulations.

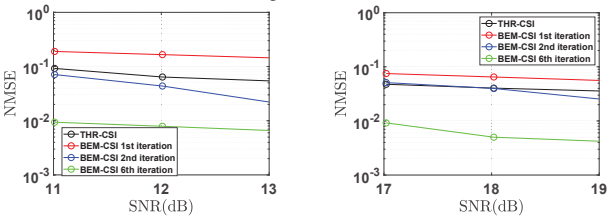

(a) QPSK,$M=128, N=32$ (b) 16-QAM,$M=64, N=60$

Fig. 3: NMSE of the channel estimation performance.

Compared to the single pilot in OTFS, the total pilot energy $E_{\rm p}$ is equally distributed over N' pilot symbols in OFDM.

Detailed system parameters are shown in Table I. The number of data symbols in an OTFS block is $L^{\rm OTFS} = (M-2M_{\rm g}-1)\times N$ and is $L^{\rm OFDM} = M \times N'$ for an OFDM block. We let the code length be $L^{\rm OTFS}$ symbols and choose N' to be the smallest integer such that $L^{\rm OFDM}$ is at least $L^{\rm OTFS}$. In our simulations, we adopt the Extended Vehicular A Model, which has $L = M_{\rm cp} = 12$ delay taps. The maximum Doppler frequency is $f_{\rm d} = 1000$ Hz, corresponding to a mobile speed of 270 km/h with 4 GHz carrier frequency.

For OTFS with threshold-based channel estimation, since it utilizes a single pilot on the DD domain for channel estimation, a high pilot power $E_{\rm p}$ is required to produce reliable channel estimates. However, when $E_{\rm p}$ is too high, the amount of power available for data transmission decreases, which degrades performance. Hence, we follow the standard practice in [2] to numerically optimize the pilot power $E_{\rm p}$ such that a good system bit-error-rate (BER) can be achieved. The optimal values of the pilot signal-to-noise power ratio (SNR) over the data SNR, written equivalently as $E_{\rm p}/E_{\rm d}$, are found to be $E_{\rm p}/E_{\rm d} = 31.8$ dB for the system with setting 1 or 2 at $E_{\rm b}/N_0 = 8$ dB, and about 33 dB for the system with setting 3 or 4 at $E_{\rm b}/N_0 = 10$ dB. We also note that if we simply allocate all the unused power in the guard band (see Fig. 1b) to the single pilot in the DD domain,$E_{\rm p}/E_{\rm d}$ is 28.7 dB and 31.4 dB, respectively; however, for these two settings, the resulting BERs become inferior. In contrast, for BEM-based channel estimation, a much lower pilot power is needed. Here, we simply set $E_{\rm p} = NE_{\rm d}$ and $E_{\rm p} = N'E_{\rm d}$ for the two systems. For the OTFS with BEM channel estimation, we have $E_{\rm p}/E_{\rm d}\ ({\rm dB}) = 10\log_{10} N$, which is 15 dB ($N=32$) for setting 1 or 2, and is 18 dB ($N=64$) for setting 3 or 4. Thus, when using BEM channel estimation instead of the threshold-based channel estimation, the reduction in pilot power is $31.8-15 = 16.8$ dB for settings 1 or 2, and is $33-18 = 15$ dB for setting 3 or 4. Note that our choice of $E_{\rm p}/E_{\rm d}$ for the BEM follows that of [3] such that in the time domain, the power of the single pilot in the pilot block (see Fig. 2) equals the power of the data symbol. We do not further increase $E_{\rm p}/E_{\rm d}$ for BEM channel estimation as the current setting achieves good channel estimation performance and the peak-to-average-power ratio (PAPR) (see Table I).

In Fig. 3, we plot the normalized mean square error (NMSE) vs. SNRs of the proposed BEM OTFS channel estimation and the threshold-based channel estimation for setting 2 and setting 4, respectively, where SNR(dB) $= E_{\rm b}/N_0$(dB) $+ 10\log_{10}(\log_2 Q)$. It is shown that while the BEM channel estimation has a higher NMSE at the first iteration (due to the use of lower transmission power on pilots), the accuracy of the BEM channel estimation improves over subsequent iterations of joint equalization and decoding. This demonstrates the benefit of using decoded symbols to improve channel estimation.

B. Performance Evaluation

In Fig. 4, we present BER curves of OTFS and OFDM systems after six iterations of joint channel estimation, equalization, and channel decoding. We consider four settings, shown in Table I, and four ways of obtaining CSI: perfect (PER) CSI Full, threshold-based (THR) CSI, BEM CSI, and PER-CSI Pilot. Here, PER-CSI Full assumes perfect knowledge of the CSI at every symbol in the DD domain, while PER-CSI Pilot is the case where only one snapshot of the channel is known at the pilot location. We introduce PER-CSI Pilot here to examine how much THR-CSI can approach the performance of PER-CSI Full. The fact that PER-CSI Pilot performs inferior to PER-CSI Full reveals the limitation of THR-CSI: it does not take into account the variation of the 2D response on the DD domain and thus causes performance degradation. BEM-CSI is refined after each iteration, whereas THR-CSI remains fixed over iterations. In Fig. 4, curves for OTFS and OFDM systems are shown in black and blue, respectively. THR-CSI and PER-CSI Pilot for an OTFS system are shown in red and green, respectively. Solid curves assume PER-CSI Full, and dashed curves assume estimated CSI. Curves labeled by circle and diamond are for MP and MMSE, respectively. The damping factor for MP is set to 0.05 for setting 1 or 2, and 0.1 for setting 3 or 4. Main observations from Fig. 4 are:

- Fig. 4 (a) assumes setting 1 with BPSK. We see that OTFS system outperforms OFDM system under both PER-CSI Full and BEM-CSI. Under BEM-CSI, OTFS with MP is about 1.6 dB better than OFDM with MMSE. Here, for OTFS, MP equalizer performs only slightly better than the MMSE. We also note that OTFS THR-CSI is about 2 dB inferior to BEM-CSI and PER-CSI Pilot. Performance improvement from 6 to 7 iterations is shown to be limited for BEM OTFS and OFDM systems.
- As shown in Fig. 4 (b), results for settings 2 with QPSK are similar to those of setting 1. OTFS with MP outperforms the OFDM system by about 1 dB and 0.3 dB under BEM-CSI and PER-CSI Full, respectively. We also observe that OTFS with MP outperforms OTFS with MMSE by about 1 dB under BEM-CSI.

This article has been accepted for publication in IEEE Wireless Communications Letters. This is the author's version which has not been fully edited and content may change prior to final publication. Citation information: DOI 10.1109/LWC.2023.3284778

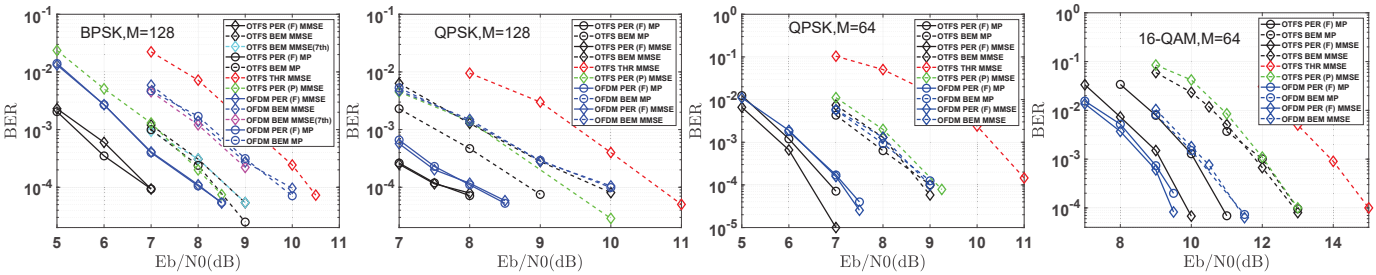

(a) $M = 128$, $N = 32$; $N' = 27$, (b) $M = 128$, $N = 32$; $N' = 27$, (c) $M = 64$, $N = 60$; $N' = 39$, (d) $M = 64$, $N = 60$; $N' = 39$,

Fig. 4: Performance comparison of coded OTFS and OFDM.

- Fig. 4 (c) considers setting 3 with a larger $N = 60$. Under BEM-CSI, the OTFS system performs only slightly better than the OFDM system, and the MP and MMSE equalizers perform comparably. Only under PER-CSI Full, OTFS with MMSE outperforms OFDM with MMSE by about 0.5 dB. The MMSE equalizer performs slightly better than MP equalizer for the OTFS system.
- Fig. 4 (d) considers setting 4 with $N = 60$ and 16-QAM modulation. For this setting, we note that the OFDM system outperforms OTFS system under both PER-CSI Full and BEM-CSI. For the latter, the performance gap is about 2 dB. We also note that for OTFS, the MMSE equalizer outperforms the MP equalizer by about 1 dB under PER-CSI Full and BEM-CSI. This suggests that a denser channel matrix causes a greater performance degradation for the MP equalizer when the larger modulation size of 16-QAM is used. On the other hand, the 2 dB performance loss of OTFS compared to OFDM shows that performance of the MMSE equalizer is limited due to the larger 2D channel spread and modulation size.

C. Complexity Analysis

In this subsection, we analyze and compare the computational complexity of the MP and soft MMSE equalizers for both OTFS and OFDM. Considering the number of complex multiplications (CMs), complexity order of the MP equalizer is $\mathcal{C}_{\text{MP}} = \mathcal{O}(MNBQI_{\text{MP}})$ [5], where I_{MP} is the number of inner iterations, B is the number of nonzero elements in each row of the channel matrix, and we choose $I_{\text{MP}} = 20$ in settings. The main contributing factor to the complexity of the soft MMSE equalizer is the channel matrix inversion. As shown in [10], the MMSE equalizer can be efficiently implemented by deploying the least squares minimum residual (LSMR) algorithm with the complexity order of $\mathcal{C}_{\text{MMSE}} = \mathcal{O}(MNBI_{\text{LSMR}})$, where I_{LSMR} is the number of the LSMR algorithm iterations. Typical value of $I_{\text{LSMR}} = 15$ provides the same performance as that of MMSE with direct matrix inversion, [10]. Similar to [10], we assume the channel coefficients on L delay taps occupy all the Doppler bins in OTFS. With this assumption, the channel matrix in OFDM is not sparse due to ICI. Therefore, $B_{\text{OTFS}} = NL$ and $B_{\text{OFDM}} = M$. For the four settings shown in Table 1, we find that for both OTFS and OFDM, the complexity order of MP is 2.5 $\sim$ 21.3 higher than MMSE, depending on the modulation size Q. When using the same equalizer (MMSE or MP), the complexity order of OTFS is about 3.5 $\sim$ 17.3 times higher than OFDM, primarily due to the larger B_{OTFS} compared to B_{OFDM}.

VI. Conclusion

This work brought OTFS and OFDM under the microscope and provided a thorough comparison of the two systems that was missing in existing literature. In this comparison, practical aspects such as limited pilot power, channel estimation, and channel coding, were taken into account while advanced equalizers were applied to both systems. A BEM based channel estimation technique was also proposed to provide more accurate channel estimates with a substantially reduced pilot power than the commonly used threshold-based channel estimator. Utilizing the proposed BEM-based channel estimator, our results show that OTFS outperforms OFDM for small modulation sizes in terms of BER. In contrast, for larger modulation sizes such as 16-QAM, OFDM shows a superior BER performance than OTFS. This is due to the challenges of 2D detection which necessitates the need for development of more advanced equalizers for OTFS to unleash the potential of this promising waveform.

References

[1] R. Hadani, S. Rakib, M. Tsatsanis, A. Monk, A. J. Goldsmith, A. F. Molisch, and R. Calderbank, "Orthogonal time frequency space modulation," in *Proc. of IEEE Wireless Communi. and Network. Conference*, 2017, pp. 1–6.

[2] P. Raviteja, K. T. Phan, and Y. Hong, "Embedded pilot-aided channel estimation for otfs in delay–doppler channels," *IEEE Transactions on Vehicular Technology*, vol. 68, no. 5, pp. 4906–4917, 2019.

[3] P. Wan, M. McGuire, and X. Dong, "Near-optimal channel estimation for ofdm in fast-fading channels," *IEEE transactions on vehicular technology*, vol. 60, no. 8, pp. 3780–3791, 2011.

[4] L. Zhao, W. Guo, Y. Liu, J. Yang, and W. Wang, "Pilot optimization for ofdm-based otfs systems over doubly selective channels," in *IEEE Global Communications Conference*, 2020, pp. 1–6.

[5] P. Raviteja, K. T. Phan, Y. Hong, and E. Viterbo, "Interference cancellation and iterative detection for orthogonal time frequency space modulation," *IEEE Transactions on Wireless Communications*, vol. 17, no. 10, pp. 6501–6515, 2018.

[6] H. B. Mishra, P. Singh, A. K. Prasad, and R. Budhiraja, "Iterative channel estimation and data detection in otfs using superimposed pilots," in *Proc. of IEEE Inter. Conf. on Commun. Workshops*, 2021, pp. 1–6.

[7] S. Li, J. Yuan, W. Yuan, Z. Wei, B. Bai, and D. W. K. Ng, "Performance analysis of coded otfs systems over high-mobility channels," *IEEE Transactions on Wireless Communications*, 2021.

[8] N. Hashimoto, N. Osawa, K. Yamazaki, and S. Ibi, "Channel estimation and equalization for cp-ofdm-based otfs in fractional doppler channels," in *Proc. of IEEE Inter. Conf. on Commun. Workshops*, 2021, pp. 1–7.

[9] A. RezazadehReyhani, A. Farhang, M. Ji, R. R. Chen, and B. Farhang-Boroujeny, "Analysis of discrete-time mimo ofdm-based orthogonal time frequency space modulation," in *Proc. of IEEE Inter. Conf. on Communication*, 2018, pp. 1–6.

[10] H. Qu, G. Liu, L. Zhang, S. Wen, and M. A. Imran, "Low-complexity symbol detection and interference cancellation for otfs system," *IEEE transactions on communications*, vol. 69, no. 3, pp. 1524–1537, 2020.